Available online at www.sciencedirect.com
ScienceDirect
Journal of Sound and Vibration 308 (2007) 845–854
JOURNAL OF SOUND AND VIBRATION
www.elsevier.com/locate/jsvi

Analysis of forces in ultrasonically assisted turning

N. Ahmed, A.V. Mitrofanov*, V.I. Babitsky, V.V. Silberschmidt

Wolfson School of Mechanical and Manufacturing Engineering, Loughborough University, LE11 3TU, UK

Accepted 2 April 2007
The peer review of this article was organised by the Guest Editor
Available online 18 May 2007

Abstract

Many modern engineering materials are very difficult to process with conventional machining methods. Ultrasonically assisted turning (UAT) is a new technology, where high frequency vibration (frequency $f \approx 20$ kHz, amplitude $a \approx 15$ μm) is superimposed on the movement of the cutting tool. Compared to conventional turning (CT), UAT allows significant improvements in processing many intractable materials, such as high-strength aerospace alloys and composites, by producing a noticeable decrease in cutting forces and a superior surface finish. Vibro-impact interaction between the tool and workpiece in UAT during the chip formation leads to a dynamically changing cutting force in the process zone as compared to the quasistatic one in CT. The paper presents an experimental study and computational (finite-element) model of both CT and UAT. Forces acting on the cutting tool in UAT are studied, and their dependence on vibration amplitude, frequency and vibration direction as well as on cutting parameters, such as feed rate and cutting speed, are investigated.

1. Introduction

Turning is a type of material processing operation where a cutting tool is used to remove an unwanted material to produce a desired product, and is generally performed on a lathe. In recent decades, considerable improvements were achieved in turning, enhancing machining of difficult-to-cut materials and producing better surface finish. Various methods, such as high-speed machining, have been in use for considerable time. However, machining of high-strength aerospace alloys, composites and ceramics causes high tool temperatures and fast wear of cutting edges, lacks dimensional accuracy and requires a considerable amount of coolant. These deficiencies of conventional turning (CT) necessitate the development of new cutting techniques.

Ultrasonically assisted turning (UAT) has brought significant benefits to machining of hard-to-cut alloys. In UAT, high-frequency vibration (frequency $f \approx 20$ kHz, amplitude $a \approx 15$ μm) is superimposed on the movement of a cutting tool. Compared to CT, this technique results in a multifold decrease in cutting forces and a considerable improvement in surface finish [1].

*Corresponding author. Tel.: +44 1509 227625; fax: +44 1509 227648.
E-mail address: a.v.mitrofanov@lboro.ac.uk (A.V. Mitrofanov).

0022-460X/$ - see front matter © 2007 Elsevier Ltd. All rights reserved.
doi:10.1016/j.jsv.2007.04.003

Despite all its advantages, this technique has not yet been widely introduced in the industry. Problems, such as instability of the cutting process resulting in poor surface finish, prevented the full implementation of its benefits. The development of an autoresonant control system [2] enhanced stability of the process by making the vibrations regular, thus providing the way to the industrial introduction of UAT.

A prototype of the UAT system has been designed at Loughborough University, UK, and a program of experimental tests has been implemented confirming advantages of UAT in comparison to CT. Dynamics of UAT as a nonlinear vibro-impact process was studied in Ref. [3], and the amplitude response of the cutting tool under loading was analysed for this cutting technique.

However, mechanics of the tool–workpiece interaction, which is of special importance for the regime with multiple microimpacts in the process zone, and other specific features of the cutting process in UAT have not been fully understood. This necessitates the use of finite element method (FEM), a main computational tool for a simulation of the process zone and tool–workpiece interaction in metal cutting. A detailed review of FE models of CT can be found in the monographs [4,5]; some recent examples are illustrated in Refs. [6–9]. These models are used to study three-dimensional (3D) forces and tool dynamic effects, thermo-mechanical coupling, constitutive damage law and contact with friction and their effect on cutting forces and plastic deformation.

A first 2D FE model of UAT was suggested in Ref. [10]: the steady state UAT process as well as processes within a single cycle of ultrasonic vibration were numerically analysed in order to understand mechanics of the tool–chip interaction under conditions of superimposed ultrasonic vibration. This initial, purely mechanical model was further improved, resulting in a transient, thermomechanically coupled one for both UAT and CT [11]. The improved model also allowed replicating the multifold reduction in cutting forces in UAT numerically that was previously obtained only experimentally. A detailed analysis of thermo-mechanics of the UAT process was further conducted in Ref. [12]. A first 3D FE model of UAT was developed as an extension of the 2D model and presented in Refs. [13,14]. The use of the 3D model allowed the study of 3D chip formation predicting distributions of stresses, strains, cutting forces and temperatures in the workpiece and cutting tool. Effects of lubrication and friction on the chip shapes and cutting forces in UAT and CT were studied [13] using both 2D and 3D FE models. The developed 3D model was also employed to analyse the workpiece material's response to ultrasonic vibration loading in Ref. [15]. Thermally induced strains and residual stresses in the surface layer of the workpiece machined with UAT and CT were investigated.

The cutting force is one of the governing parameters defining efficiency of the cutting process. A reduction in the cutting force would result in the extension of the tool life, improved surface finish and roundness of machined workpieces, as well as allow an increase in the material removal rate, i.e. in the amount of the material removed in unit time. This paper describes experimental results obtained on our in-house UAT prototype as well as respective computational results related to cutting forces obtained with the 3D FE model of UAT [16].

2. Experimental results

Experimental measurements of the cutting force are performed with a piezoelectric Kistler dynamometer (KIAG SWISS Type 9257A) that is fixed to the cross-slide of the lathe with the ultrasonic system mounted on its top (Fig. 1). High rigidity of the system ensures measurements practically without displacement; thus the dynamometer does not noticeably affect the stiffness of the tool–workpiece system. The cut-off frequency of the built-in filter is 200 Hz, consequently leading to the elimination of the high-frequency component of the force during turning. Hence, the force measured with the dynamometer represents a mean value, which in the case of UAT is averaged over a large number of cycles of ultrasonic vibration. The main component of the cutting force, coinciding in this case with the direction of ultrasonic vibration, is considered to compare CT and UAT.

The following cutting conditions are used in the tests: depth of cut $a_p = 0.1$–0.3 mm, feed rate $s = 0.03$–0.1 mm rev^{-1}, and cutting speed $V_C = 5$–16 m min^{-1}. The workpiece material is aged Inconel 718, cutting tools used are tungsten carbide inserts (DCMT 11T304 supplied by Sandvik Coromant), and Electrolube HDC400 cutting fluid is applied in the cutting region.

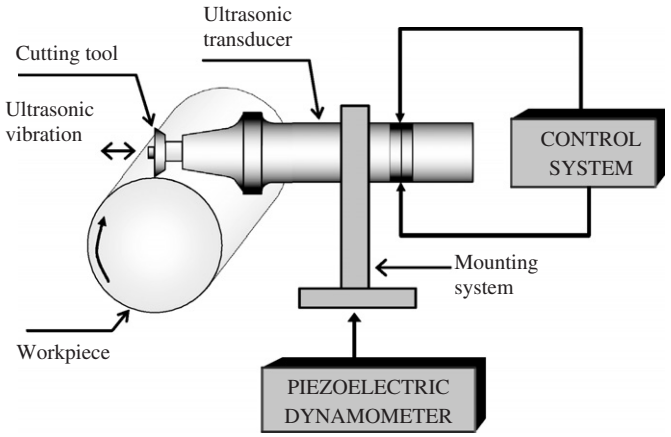

Fig. 1. A schematic diagram of the experimental setup.

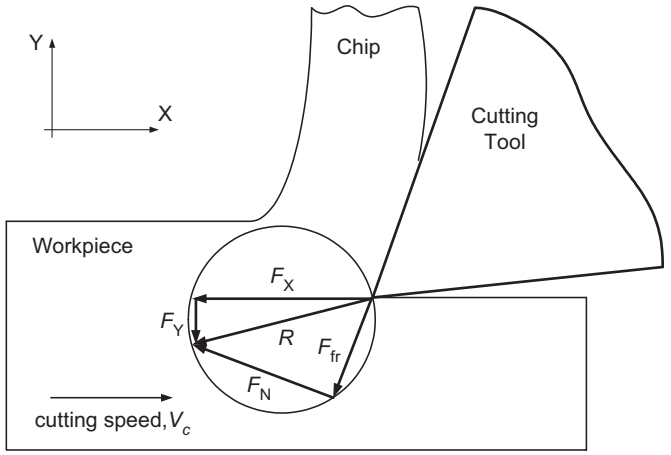

Fig. 2. Merchant's force circle.

Table 1
Cutting forces in CT and UAT of Inconel 718 for different feed rates ($a_p = 0.1$ mm, $V_C = 5\,\mathrm{m\,min^{-1}}$, turning with lubricant)

s, mm rev^{-1}	F_{CT}, N	F_{UAT}, N	F_{UAT}/F_{CT}
0.03	120	30–40	0.25–0.33
0.05	170	100	0.59
0.08	205	120	0.59
0.1	255	160	0.63

The forces in cutting can be represented with the Merchant's force circle (Fig. 2). The resultant force R can be resolved into components acting along different axes. Firstly, it can be obtained as a combination of the main cutting force F_X and feed force F_Y. Secondly, it can be projected onto the rake face and normal to the rake face directions, becoming a combination of friction force F_{fr} and normal force F_N on the rake face of the tool. In our experiments and FE calculations, the main cutting force F_X is analysed.

A dependence of the cutting force on the feed rate in turning is studied. The following cutting conditions are used in these tests: $a_p = 0.1$ mm, $V_C = 5\,\mathrm{m\,min^{-1}}$. The measured cutting force in UAT (F_{UAT}) is invariably much lower than the cutting force in CT (F_{CT}). The ratio F_{UAT}/F_{CT} is considerably lower at the low feed rate (0.25–0.33), and stabilizes at about 0.6 at higher feed rates. With an increase in the feed rate from 0.03 to

0.1 rev min^{-1}, the cutting force in CT doubles, whereas that in UAT grows about fivefold (Table 1), but still remains much lower than F_{CT}. The increase in the cutting force with a growth in the feed rate is obviously explained by an increase in the tool load at higher material removal rates. The difference in the ratio F_{UAT}/F_{CT} for the lowest and highest feed rates can be attributed to the decrease in amplitude of ultrasonic vibration due to the increased load acting on the tool.

The influence of the lubrication on the cutting force is also studied. The following cutting conditions are used in this series of experiments: $a_p = 0.2$ mm, $s = 0.03$ mm rev^{-1}, $V_C = 5$–10 m min^{-1}. The average reduction in the cutting force with application of the lubricant onto the surface of the workpiece for UAT was about 30%, which was about double the reduction observed for CT. The ratio F_{UAT}/F_{CT} in dry turning was about 0.2 and 0.33 for $V_C = 5$ and 10 m min^{-1}, respectively.

The influence of the cutting speed on the cutting forces is also experimentally analysed. With an increase in V_C from 5 to 15 m min^{-1}, the force in CT decreases from 140 to 130 N, whereas the force in UAT grows from 60 to 95 N. A drop in the force in CT could be explained by the lower fracture toughness of the workpiece material at higher strain rates resulted from greater cutting speeds. The growing force in UAT is caused by the increased time of the contact between the cutting tool and chip, with the cutting speed getting closer to its critical value ($V_t = 2\pi af$).

3. FE model description

The current FE model utilizes the MSC MARC/MENTAT finite element code [17] and is based on the updated Lagrangian analysis procedure that provides a transient analysis for an elasto-plastic material and accounts for the frictional contact interaction between the cutter and workpiece as well as material separation in front of the cutting edge.

3.1. Geometry, kinematics and FE mesh

A 3D model for the orthogonal turning process, i.e. the one where the tool edge is normal to both the cutting and feed directions, is considered. The dimensions of the part of the workpiece modelled in simulations

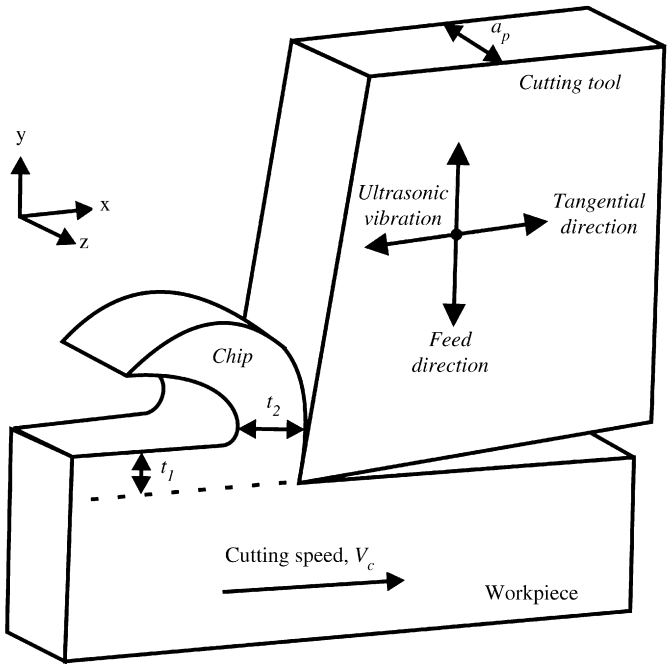

Fig. 3. A scheme of the relative movement of the workpiece and cutting tool in 3D simulations of UAT.

are 2.5 mm in length × 0.5 mm in height × 0.4 mm in depth with the uncut chip thickness $t_1 = 0.1$ mm (see Fig. 3). It is worth noting that t_1 corresponds to feed rate s in experiments. The relative movement of the workpiece and cutting tool in CT is simulated by the translation of the tool with the constant velocity $V_C = 20\,\mathrm{m\,min^{-1}}$. Harmonic oscillation with vibration amplitude $a = 15\,\mu\mathrm{m}$ (peak-to-valley) and frequency $f = 20\,\mathrm{kHz}$ is then superimposed on this movement either in the tangential or feed direction (i.e. along X-axis or Y-axis, respectively, in Fig. 3) in order to model ultrasonic vibration of the tool:

$$u = -a\cos\omega t, \tag{1}$$

where $\omega = 2\pi f$.

Hence, the vibration velocity is described by the relation:

$$\dot{u} = V_t \sin\omega t, \tag{2}$$

where $V_t = 2\pi af \approx 113\,\mathrm{m\,min^{-1}}$. Thus $V_t > V_C$, providing a condition for separation of the cutter from the chip within each cycle of ultrasonic vibration. It transforms the cutting process into the one with multiple-impact interactions between the tool and chip. Various stages of a vibration cycle are described in detail in Ref. [18].

The cutting tool is modelled as a rigid body and consists of 512 eight-node hexagonal elements with thermal properties of tungsten carbide. The workpiece is divided into about 1000 first-order tetrahedral elements in simulations. Automatic remeshing is used in the workpiece and chip to update the mesh during simulations, as otherwise some elements would become highly distorted that would affect the accuracy of the solution. The initial FE mesh and that with the fully formed chip are shown in Fig. 4a and b, respectively.

3.2. Material model

The mechanical behaviour of the workpiece material (aged Inconel 718) is described in FE simulations by the Johnson-Cook material model [19] that accounts for nonlinear material hardening and strain-rate sensitivity:

$$\sigma_Y = (A + B\varepsilon_p^n)\left(1 + C\ln\left(\frac{\dot{\varepsilon}_p}{\dot{\varepsilon}_0}\right)\right)(1 - T^{*m}), \tag{3}$$

where $A = 1241\,\mathrm{MPa}$, $B = 622\,\mathrm{MPa}$, $C = 0.0134$, $n = 0.6522$, ε_p and $\dot{\varepsilon}_p$ are plastic strain and plastic strain rate, $T^* = (T - T_{\mathrm{room}})/(T_{\mathrm{melt}} - T_{\mathrm{room}})$, T_{room} and T_{melt} are the room and melting temperatures, respectively.

A term T^{*m} is assumed to be negligible since thermal softening of Inconel 718 is insignificant (less then 5%) within the temperature range that is obtained in both our FE simulations and infrared thermography experiments for chosen cutting parameters. This material model, utilized by various researchers (see, e.g. [20,21]), has been modified to prevent unrealistically high stress values at high strains, so that maximum stress values are limited to ultimate tensile strength of Inconel 718 at corresponding strain rates (that can reach $10^5\,\mathrm{s^{-1}}$ in studied cases).

The developed FE model is fully thermomechanically coupled in order to properly reflect interconnection between thermal and mechanical processes in the cutting zone: excessive plastic deformation and friction at

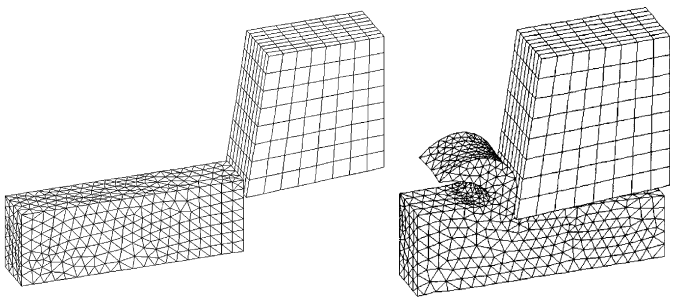

(a) (b)

Fig. 4. 3D simulations of chip formation: initial mesh (a) and fully formed chip with remeshed mesh (b).

the tool–chip interface lead to high temperatures generated in the cutting region. This results in thermal stresses and volumetric expansion as well as affects material properties of the workpiece, such as thermal conductivity and specific heat. More details on thermomechanical processes in UAT in comparison to CT can be found in Ref. [12].

3.3. Friction model

High contact stresses are generated at the tool–chip interface leading to significant friction forces. The classical Coulomb model is unable to adequately reflect friction processes under these conditions thus resulting in unrealistically high friction forces. Hence, the shear friction model [17] was chosen for simulations, where the friction force depends on the fraction of the equivalent stress of the material and not the normal force as in the Coulomb model. Thus, the friction stress is introduced in the following form:

$$\sigma_{\mathrm{fr}} \leqslant -\mu \frac{\bar{\sigma}}{\sqrt{3}} \frac{2}{\pi} \operatorname{sgn}(V_r) \arctan\left(\frac{V_r}{V_{\mathrm{cr}}}\right), \tag{4}$$

where $\bar{\sigma}$ is the equivalent stress, V_r is a relative sliding velocity, V_{cr} is a critical sliding velocity below which sticking is simulated, μ is a friction coefficient, and sgn(x) is the signum function.

Two contact conditions are considered at the tool–chip interface: (a) a frictionless contact, and (b) a contact with friction (coefficient of friction $\mu = 0.5$). The former case corresponds to the idealized condition where heat generation occurs only due to plastic deformation processes; it can be considered as an extreme case of friction reduction due to lubrication. Case (b) models dry cutting conditions, with an additional heat source due to friction between the tool surface and separated workpiece material.

3.4. Model capabilities

The current model enables us to study the influence of vibration parameters (i.e. frequency and amplitude) on the process variables (e.g. stresses, strains, temperatures and cutting forces). The effect of various vibration directions of the tool on the cutting process can also be analysed. An obvious advantage of the 3D finite-element model is its capability to study various combinations of vibration directions, whereas their experimental implementation can be extremely laborious, as it may require new types of ultrasonic transducers and mounting systems to be designed. Furthermore, the 3D FE formulation helps to perform a direct comparison of numerical results with experimental tests for oblique cutting, thus not requiring any changes to a standard cutting setup. The model also allows for oblique chip formation and chip's expansion in the lateral dimension (along Z-axis in Fig. 3). Finally, the real geometry of the cutting tool is naturally implemented in the 3D model, thus allowing the analysis of the influence of the tool geometry and wear on the cutting process with ultrasonic vibration.

4. Results of FE simulations and discussion

All numerical (finite element) simulations below are performed for two machining techniques (CT and UAT) with identical cutting parameters so that results for CT could serve as a reference for UAT.

A significant difference in forces acting on the cutting tool is obtained for UAT and CT. In simulations of CT the force acting on the cutting tool remains practically unchanged, whilst in UAT simulations it changes drastically within each cycle of vibration. The cutting force grows steadily from the moment of the first contact between the vibrating tool and formed chip until it reaches the maximum level at the point of maximum penetration. This maximum force is by 30% higher than the average force in CT. The force magnitude then starts to decline at the unloading stage until it vanishes when the cutter separates from the chip and starts to move away from it. The forces stay close to zero level until the cutter comes into contact with the chip again at the next cycle of ultrasonic vibration. The comparison of values from Fig. 5 shows that the force in UAT (averaged over the vibration cycle) is about 40% of that in CT. Low-level fluctuations of the cutting force at the withdrawal and approach stages of the cycles are explained by the remaining contact between the cutter and freshly formed workpiece surface, as well as by the numerical error involved in FE simulations.

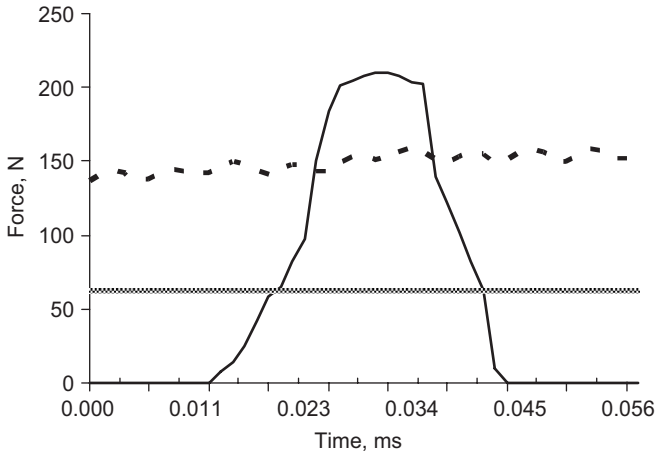

Fig. 5. Comparison of force acting on the cutting tool in the cutting direction for CT and UAT simulations ($f = 20$ kHz, $a = 15$ μm, $\mu = 0.5$). --- CT; ———— UAT; average UAT level.

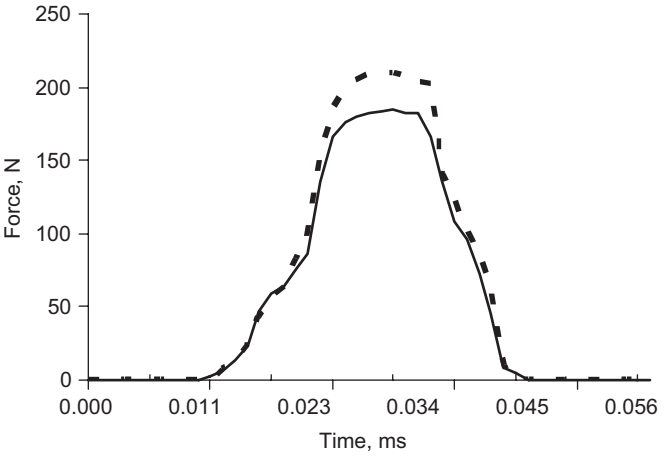

Fig. 6. Comparison of force acting on the cutting tool for UAT in the cutting direction with friction ($\mu = 0.5$) and without friction. ———— $\mu = 0$; --- $\mu = 0.5$.

A difference in forces acting on the cutting tool is also obtained in simulations of UAT with and without friction (Fig. 6). The maximum magnitudes of cutting forces are reached when the tool is in full contact with the chip, with these forces dropping to zero levels when the tool disengages from the chip. The maximum magnitude of the cutting force in simulations with friction is by 20–25% higher than that in frictionless simulations. This result is in good agreement with our experimental measurements, showing 25% reduction in the cutting force in UAT when the lubricant is applied (see Section 2).

FE simulations are conducted to study the effect of vibration amplitude and frequency on the force acting on the cutting tool in UAT. An increase in the peak force with an increase in amplitude is observed (Fig. 7), however, an average cutting force decreases. This is explained mainly by the increase of the relative velocity of the cutting tool resulting in a shorter period of contact with a chip for a given frequency (i.e. period) of ultrasonic vibration. A decrease of 28% in the average force is recorded for an increase in the amplitude from 7.5 to 15 μm, and a further 24% decrease is observed when the amplitude increases from 15 to 30 μm (Fig. 7b).

In the analysis of the frequency's influence on the cutting force, the peak force remains nearly at the same level in all studied cases, but the average force decreases by 21% for a frequency increase from 10 to 20 kHz (Fig. 8). A further 26% decline in the average force is observed when vibration frequency increases from 20 to

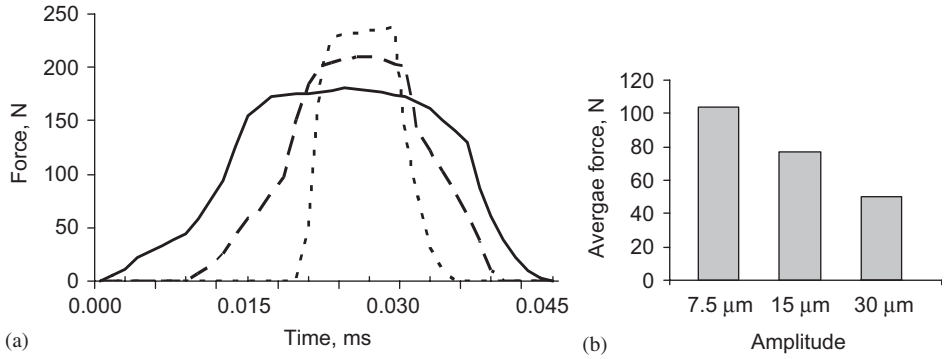

Fig. 7. Effect of vibration amplitude on forces in cutting tool: (a) evolution of force, and (b) average cutting force ($f = 20$ kHz, $\mu = 0.5$). Vibration amplitudes: ——— 7.5 μm; – – – 15 μm; - - - - 30 μm.

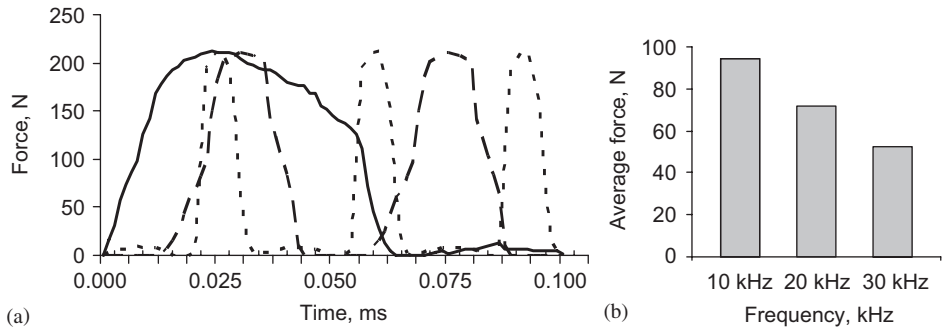

Fig. 8. Effect of ultrasonic frequency on forces in cutting tool: (a) evolution of force, and (b) average cutting force ($a = 15$ μm, $\mu = 0.5$). Ultrasonic frequency: ——— 10 kHz; – – – 20 kHz; - - - - 30 kHz.

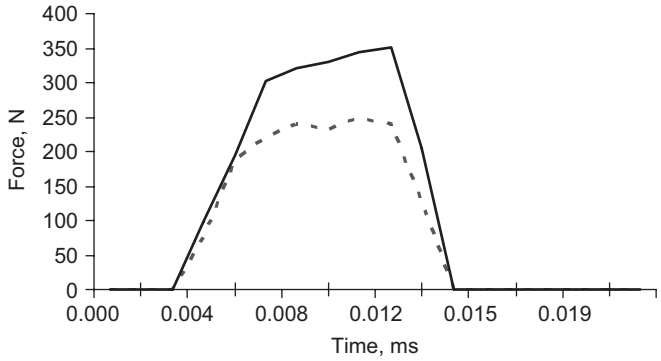

Fig. 9. Effect of feed rate on forces in the cutting tool ($f = 20$ kHz, $a = 15$ μm, $\mu = 0.5$). Feed rate: - - - - 0.1 mm; ——— 0.2 mm.

30 kHz. This trend can be explained by the increase in the velocity of the vibrating cutting tool, which amplitude is proportional to both vibration amplitude and frequency (see Eq. (2)).

The cutting parameters corresponding to the typical combination of vibration parameters used in our experiments with UAT ($f = 20$ kHz, $a = 15$ μm) are also investigated. Two different feed rates $s = 0.1$ and 0.2 mm are compared. It has to be pointed out that some smaller feed rates used in the experimental tests ($s = 0.03$–0.08 mm) could not be analysed with the current FE model due to the limitation on the minimum element size. Fig. 9 shows that whilst the character of the force evolution during the cycle stays the same for both feed rates, an increase in the feed rate from 0.1 to 0.2 mm (i.e. a two-fold increase in the material removal rate) leads to a 40% growth in the maximum force magnitude.

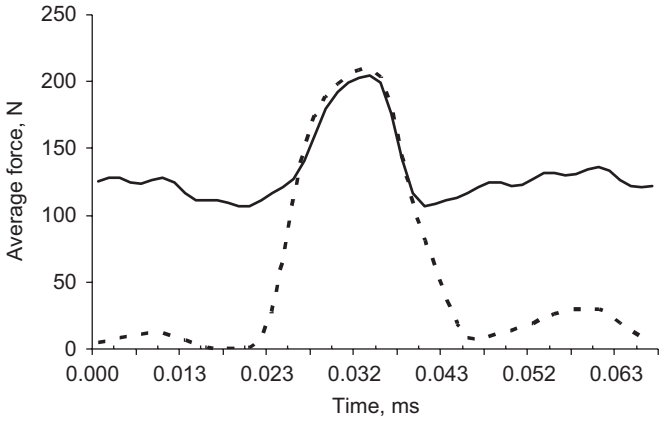

Fig. 10. Influence of vibration direction on forces in the cutting tool ($f = 20$ kHz, $a = 15$ μm, $\mu = 0.5$). ———— vibration in the feed direction; …… vibration in the tangential vibration.

Cutting forces are compared in simulations of UAT with ultrasonic vibration applied in the tangential or in the feed direction (see Fig. 10). When ultrasonic vibration is applied in the feed direction, there is no separation between the cutting tool and chip within every cycle of vibration, as it was in the case of tangential vibration; instead, separation between the tool and workpiece (along Y-axis in Fig. 3) takes place. In this case, when the tool is not in contact with the workpiece, the average cutting force is equal to about 120 N. Once the tool comes into contact with the workpiece, the force rises to about 200 N and stays at that level until the tool loses contact with the workpiece at the next cycle of vibration. The mean cutting force over the cycle of ultrasonic vibration is 130 N in case of feed vibration, as compared to 50 N for tangential vibration. Hence, tangential vibration leads to a greater force reduction in UAT, thus it can be more beneficial for the cutting process. Still, the final conclusion on the efficiency of vibration directions cannot be based only the force comparison, as other factors, e.g. the quality of the machined surface, should be analysed.

5. Conclusions

The cutting forces in ultrasonically assisted turning (UAT) are analysed with computational and experimental methods, with conventional turning (CT) being a basis of comparative analysis. A 3D finite-element (FE) model allows calculations of the effects of vibration frequency and amplitude, feed rate and friction on the cutting force. An increase in the vibration amplitude from 7.5 to 30 μm in FE simulations leads to a 52% decrease in the average cutting force in UAT that could be explained by an increased part of a cycle of ultrasonic vibration without a contact between the tool and chip. An increase in the vibration frequency from 10 to 30 kHz results in a 47% drop in the level of average cutting forces, which could be attributed to an increased velocity of the tool vibration. Hence, an increase in either vibration frequency or amplitude leads to a decrease in cutting forces in the UAT process that is beneficial to increasing the accuracy of the cutting process and improving material removal rates. Calculations also show that vibration in the tangential direction causes the lower cutting force than that obtained with vibration in the feed direction.

For the typical combination of vibration parameters ($f = 20$ kHz, $a = 15$ μm) the calculated cutting force in UAT is 40% of that in CT, whilst the experimental measurements showed that the force in UAT was 0.25–0.6 of that in CT for various feed rates. The comparison of feed rates indicates a 40% increase in the level of cutting forces in simulations of UAT for doubling a feed rate from 0.1 to 0.2 mm due to a higher material removal rate in the latter case. Experimental results show a 60% increase in the cutting force in UAT when the feed rate doubles from 0.05 to 0.1 mm rev^{-1}, hence we can conclude a fair agreement between experimental and numerical results. The comparison of simulations with and without friction, corresponding to dry and lubricated turning conditions, respectively, shows that in the latter case the cutting force is by 20–25% lower being in a good agreement with experimental results indicating 30% decrease in the cutting force when the lubricant was applied.

Acknowledgements

Authors would like to acknowledge the help of Dr. Alan Meadows in conducting force measurements on the UAT prototype system.

References

[1] V. Babitsky, A. Kalashnikov, A. Meadows, A. Wijesundara, Ultrasonically assisted turning of aviation materials, *Journal of Materials Processing Technology* 132 (2003) 157–167.
[2] V.I. Babitsky, A. Kalashnikov, F. Molodtsov, Autoresonant control of ultrasonically assisted cutting, *Mechatronics* 14 (2004) 91–114.
[3] V.K. Astashev, V.I. Babitsky, Ultrasonic cutting as a nonlinear (vibro-impact) process, *Ultrasonics* 36 (1998) 89–96.
[4] T.H.C. Childs, K. Maekawa, T. Obikawa, Y. Yamane, *Metal Machining: Theory and Applications*, Arnold, London, 2000.
[5] E.M. Trent, P.K. Wright, *Metal Cutting*, Butterworth-Heinemann, London, 2000.
[6] A.U. Anagonye, D.A. Stephenson, Modeling cutting temperatures for turning inserts with various tool geometries and materials, *Journal of Manufacturing Science and Engineering (Trans. ASME)* 124 (2002) 544–552.
[7] E. Ceretti, M. Lucchi, T. Altan, FEM simulation of orthogonal cutting: serrated chip formation, *Journal of Materials Processing Technology* 95 (1999) 17–26.
[8] O. Pantale, J.L. Bacaria, O. Dalverny, R. Rakotomalala, S. Caperaa, 2D and 3D numerical models of metal cutting with damage effects, *Computational Methods for Applied Mechanical Engineering* 193 (2004) 4383–4399.
[9] J.S. Strenkowski, A.J. Shih, J.C. Lin, An analytical finite element model for predicting three-dimensional tool forces and chip flow, *International Journal of Machine Tools & Manufacture* 42 (2002) 723–731.
[10] A.V. Mitrofanov, V.I. Babitsky, V.V. Silberschmidt, Finite element simulations of ultrasonically assisted turning, *Computational Materials Science* 28 (2003) 645–653.
[11] A.V. Mitrofanov, V.I. Babitsky, V.V. Silberschmidt, Finite element analysis of ultrasonically assisted turning of Inconel 718, *Journal of Materials Processing Technology* 153–154 (2004) 233–239.
[12] A.V. Mitrofanov, V.I. Babitsky, V.V. Silberschmidt, Thermomechanical finite element simulations of ultrasonically assisted turning, *Computational Materials Science* 32 (2004) 463–471.
[13] A.V. Mitrofanov, N. Ahmed, V.I. Babitsky, V.V. Silberschmidt, Effect of lubrication and cutting parameters on ultrasonically assisted turning of Inconel 718, *Journal of Materials Processing Technology* 162–163 (2005) 649–654.
[14] N. Ahmed, A.V. Mitrofanov, V.I. Babitsky, V.V. Silberschmidt, Finite element modeling of ultrasonically assisted turning, *Eighth CIRP International Workshop on Modeling of Machining Operations*, Chemnitz, Germany, 2005, pp. 107–114.
[15] N. Ahmed, A.V. Mitrofanov, V.I. Babitsky, V.V. Silberschmidt, Analysis of material response to ultrasonic vibration loading in turning Inconel 718, *Materials Science and Engineering A* 424 (2006) 318–325.
[16] N. Ahmed, A.V. Mitrofanov, V.I. Babitsky, V. Silberschmidt, 3D finite element analysis of ultrasonically assisted turning, *Computational Materials Science* 39 (2007) 149–154.
[17] MSC, *Marc User's Guide, Version 2005*, MSC Software Corporation, Los Angeles, 2005.
[18] V.I. Babitsky, A.V. Mitrofanov, V.V. Silberschmidt, Ultrasonically assisted turning of aviation materials: simulations and experimental study, *Ultrasonics* 42 (2004) 81–86.
[19] G. Johnson, W. Cook, Fracture characteristics of three metals subjected to various strains, strain rates, temperatures and pressures, *Engineering Fracture Mechanics* 2 (1985) 31–48.
[20] P. Maudlin, M. Stout, Metal cutting simulation of 4340 steel using an accurate mechanical description of material strength and fracture, *Minerals, Metals and Materials Society* (1996) 29–41.
[21] E.-G. Ng, T. El-Wardany, M. Dumitrescu, M. Elbestawi, Physics-based simulation of high speed machining, *Machining Science and Technology* 6 (2002) 301–329.